Engineered Science
DOI: https://dx.doi.org/10.30919/es8d810

Piezoelectrets From Cyclic Olefin Copolymers with Different Mechanical and Thermomechanical Properties: A Comparative Study

Hui Wang,[1, 2] Xiaolin Wang,[1, 2] Yan Li,[1, 2] Zhe Liu,[1, 2] Muhammad F. Ahmed,[1, 2] Xiaoqing Zhang[3] and Changchun Zeng[1, 2,*]

Abstract

This paper reports on the fabrication and characterization of piezoelectrets using three types of cyclic olefin copolymers (COCs). The COCs (COC 6017, 6013, 8007) differ considerably in their glass transition temperatures, thermal stability, and mechanical flexibility. The piezoelectrets were fabricated using a carbon dioxide-assisted assembly of a multi-layer non-overlapping structure followed by contact charging. The piezoelectricity was characterized by quasi-static piezoelectric coefficients. Piezoelectrets from the three COCs all showed excellent piezoelectric activity with the quasi-static piezoelectric coefficient reaching up to 1600 pC/N. The thermal stability of the three types of piezoelectret was investigated by thermally stimulated discharge (TSD). The discharge peaks for 6017, 6013, and 8007 were found to be around 210 ºC, 180 ºC, and 130 ºC, respectively. The electrical and electromechanical characteristics of the piezoelectrets were further probed by electric hysteresis loop measurements, butterfly loop measurements, and dielectric resonance spectra for all three types of materials. The study provided the first systematic and comprehensive investigation of the potential of the family of COC copolymers in piezoelectric applications, broadening the materials choices and design space of porous polymer-based piezoelectric materials.

Keywords: Piezoelectret; Cyclic olefin copolymers; Piezoelectric coefficient; Electromechanical properties; Thermal stability.
Received: 23 February 2022; Revised: 18 April 2022; Accepted: 21 April 2022.
Article type: Research article.

1. Introduction

As a type of smart material,[1-4] piezoelectric material develops electric charges in response to mechanical stresses, thereby converting mechanical energy to electrical energy. The most commonly used piezoelectric materials are piezoelectric ceramics such as lead zirconate titanate (PZT)[5-7] and Barium titanate ($BaTiO_3$).[8,9] Piezoelectric foams or piezoelectret are charged porous polymers showing piezoelectricity. In 1989, polymer piezoelectrets were first investigated in Finland.[10] Compared to traditional piezoelectric materials, piezoelectrets have significantly higher flexibility, lower toxicity, lighter weight, and lower cost, and are suitable for mass production.

To expand their application areas, a great deal of effort has gone into improving the thermal stability of the piezoelectrets by using polymers with high thermal stability, e.g., polyethylene terephthalate (PET),[11,12] polyetherimide (PEI),[13,14] polycarbonate (PC),[13,15] polyethylene naphthalate (PEN),[16-19] fluorinated ethylene propylene (FEP),[20-29] polyethylene (PE),[30] polytetrafluoroethylene (PTFE).[23,31,32] Modifications of polypropylene (PP),[33-39] the most commonly used material for piezoelectrets, were also conducted to improve its relatively low working temperature.[37,40,41] Despite making progress, success in achieving piezoelectrets with good combinations of piezoelectricity, thermal stability, and mechanical properties has been limited.

Cyclic olefin copolymers (COCs) are a group of copolymers of ethylene and a comonomer, typically norbornene. They possess excellent mechanical properties, and dielectric properties (high resistivity, low dielectric

[1] *Department of Industrial and Manufacturing, FAMU-FSU College of Engineering.*
[2] *High-Performance Materials Institute, Florida State University, Tallahassee, FL 32310, USA.*
[3] *School of Physics Science and Engineering, Tongji University, Shanghai 200092, China.*
**Email:* zeng@eng.famu.fsu.edu (C. Zeng)

constant, and dielectric losses) and demonstrate good charge storage capability, particularly for positive charges.[42] Several studies on COC piezoelectrets had been reported.[43-47] The mechanical and thermal-mechanical properties of a particular COC polymer depend on the norbornene content. A higher norbornene percentage results in a higher glass transition temperature and improved thermal stability, but more brittle material. On the other hand, a COC with a lower norbornene faction is more flexible but has a lower glass transition temperature. Thus, they may be suitable for different applications.

In this study, piezoelectrets with the same structures were fabricated using three COCs that differed in their mechanical and thermomechanical properties. Characteristics and performance of these piezoelectrets were studied, including piezoelectric coefficient, thermal stability, charge build-up process, and actuation behaviors. Additional electromechanical properties investigations on the materials were conducted using dielectric resonance spectroscopy. The study provided the first systematic and comprehensive investigation of the potential of the family of COC copolymers in piezoelectric applications, thereby broadening the materials choices and design space of porous polymer-based piezoelectric materials and providing general guidance in their fabrication and suitable application conditions.

2. Materials and Methods

2.1 Materials

TOPAS advanced polymers company supplied the cyclic olefin copolymers (COCs), grade 8007, 6013, and 6017, which have glass transition temperatures of 78°C, 138°C, and 178°C, respectively. Table 1 shows the comparison of the mechanical and thermal properties of the three COCs. COC 6017 has the highest heat deflection temperature and tensile modulus but has the lowest tensile strength and elongation at break. It is the most thermally stable but the most brittle among the three COCs. By comparison, COC 8007 has a slightly lower tensile modulus and substantially lower heat deflection temperature, but higher tensile strength and elongation at break, which is greater than 400% higher than COC 6017. It is a significantly more flexible material. COC 6013 has properties in between those of 6017 and 6013.

Table 1. Mechanical and thermal properties of COC.[48]

Property	8007	6013	6017
Tensile strength (MPa)	63	63	58
Elongation at break (%)	10	2.7	2.4
Tensile Modulus (MPa)	2600	2900	3000
Relative Permittivity	2.35	2.35	2.35
Heat deflection temperature (OC)	75	130	170

2.2 Preparation of COC piezoelectret

Fabrication of the COC piezoelectrets was previously discussed in detail,[49,50] so is only briefly described here. The process involved three steps: Fabrication of the multi-layer non-overlapping structures by laser machining, assembly/fusion of the multiple layers using carbon dioxide, and contact charging.

Piezoelectrets from the three COCs materials were fabricated using an identical structure design. Fig. 1a shows the schematic view of the prepared porous structure. Fig. 1b shows the cross-section of the non-overlapping structure before and after compression. The structure had five layers. The top, middle, and bottom layers were solid films, while the other two contains regularly spaced rectangular channels with a 3mm width generated by laser machining. The position of the channels in the two layers was offset such that the ridge of one layer was situated in the middle of the rectangular cavity in the underneath layer. The top and bottom layers were 101.6 μm thick, and the other 3 layers were 50.8 μm thick. The channel (cavity) width was 3mm, with a ridge width of 1mm.

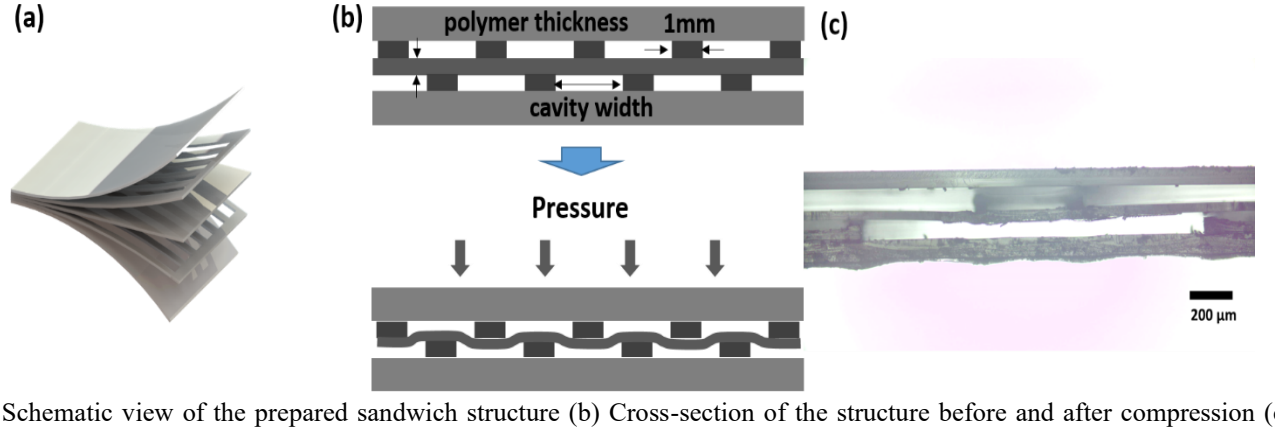

Fig. 1 (a) Schematic view of the prepared sandwich structure (b) Cross-section of the structure before and after compression (c) Optical image of COC 6013 piezoelectret. Optical images for other COCs were similar.

Such a design was rather effective in achieving low compression modulus of the structure by utilizing the bending of the middle layer at multiple locations and generation of large flexural deformation.[49,50] Since the piezoelectric coefficient is inversely proportional to the elastic modulus,[51,52] This design would facilitate a significant increase in the piezoelectric activity.

The 5-layer structure was assembled using our previously developed supercritical CO_2 bonding technology. A bonding temperature of 120 °C was chosen for COC 6017, which is approximately 60 °C lower than the glass transition temperature (178 °C) of the material. For COC 6013, for which the glass transition temperature is 138 °C, the bonding temperature was 95 °C. For COC 8007, the bonding temperature was 35 °C. The supercritical CO_2 pressure was 10 MPa for all the materials. Supercritical CO_2 can significantly reduce both the bulk and surface glass transition temperature of the polymer, as well as increase the interfacial wetting, diffusion, and randomization to forge a bonding interface, enabling polymer films easy to be bonded together.[53,54] This approach enables the porous structure to be assembled with the structural features largely preserved. As an example, Fig. 1c shows the optical image of the piezoelectret from COC 6013. The top left and bottom right areas were rectangular channels. The rectangle shape was well preserved with little deformation.

In the third step, contact charging was used to charge the prepared structure after electrodes (2 × 2 cm^2) were sputter coated onto both sides. For the samples prepared for measuring the quasi-static piezoelectric coefficient and thermally stimulated discharge spectra, the charging voltage used was 5000 V. Different charging voltages in a range from 500 V to 7500 V were applied for hysteresis loop characterization. The contact charging equipment used was Heinzinger PNC 1000-6 ump.

2.3 Quasi-static piezoelectric coefficient

Quasi-static piezoelectric coefficient measurement is a typical method to determine the sensitivity of the material. The quasi-static piezoelectric coefficient was determined by

$$d_{33} = \frac{Q}{F} = \frac{\sigma}{p} \quad (1)$$

where d_{33} is the quasi-static piezoelectric coefficient, Q is the amount of charge, F is applied force, $\boldsymbol{\sigma}$ is charge density, and p is applied pressure.

In this study, a pressure from 2.45kPa to 24.5kPa was applied to the sample, and the induced charge was measured by an electrometer (Keithley 6517A). A preload of 1.225kPa was first applied to the sample to eliminate the air gap between the sample and electrode.

2.4 Thermally stimulated discharge-current spectra

The thermal stability of the prepared samples was characterized by thermally stimulated discharge (short circuit TSD spectra).[40,55] The temperature range was from room temperature to 240 °C with a ramping speed of 3 °C/min in a temperature-controlled oven. Both sides of the sample were sputter coated with metal electrodes (2 × 2 cm^2). The thermally stimulated current was recorded by an electrometer (Keithley 6517A).

2.5 Dielectric resonance spectra

The dielectric resonance spectrum of the piezoelectret of the three types of materials was investigated at a frequency range from 0 to 1000kHz to obtain the anti-resonance frequency of the materials to calculate the elastic modulus (TE mode) of the material governed by the following relationship.[38,56]

$$f_a = \frac{1}{2s}\sqrt{\frac{Y}{\rho}} \quad (2)$$

where ρ, s, f_a and Y is the bulk modulus of the material, sample thickness, anti-resonance frequency, and material elastic modulus, respectively. The dielectric spectrum testing equipment was Agilent 4294 precision impedance analyzer.

2.6 Electrical hysteresis loop and butterfly loop

The hysteresis loop was used to investigate the charge or 'macro-dipole' build-up process in the artificial void. Precision Premier II (RADIANT) connected to a high-voltage interface was used to characterize the hysteresis loop. The bias-applied voltages ranging from 500 V to 7500 V were applied to the sample coated with metal electrodes on both sides. The equipment setup was also used for the butterfly loop measurements, which can characterize the material actuation behavior. Samples were applied with a bipolar drive voltage at a maximum value of 8000 V. Small deformations of the material were then measured by a high-precision optical fiber system (TF Analyzer 2000 system).

3. Results and discussion

3.1 Piezoelectric activity of COC piezoelectrets

Figure 2 shows the results of the measured quasi-static piezoelectric coefficient (d_{33}) of the three types of COC piezoelectrets. All displayed good piezoelectric activity. d_{33} reached 1000-1600pC/N at low pressures. Although the piezoelectric activity decreased with increasing pressure, d_{33} retained respectable values at high pressures. Among the three COC piezoelectrets, 6017 and 6013 demonstrated very similar

behaviors. While 8007 appeared to have slightly lower d_{33}, it is plausible that the piezoelectric activity was comparable to those of 6013 and 6017.

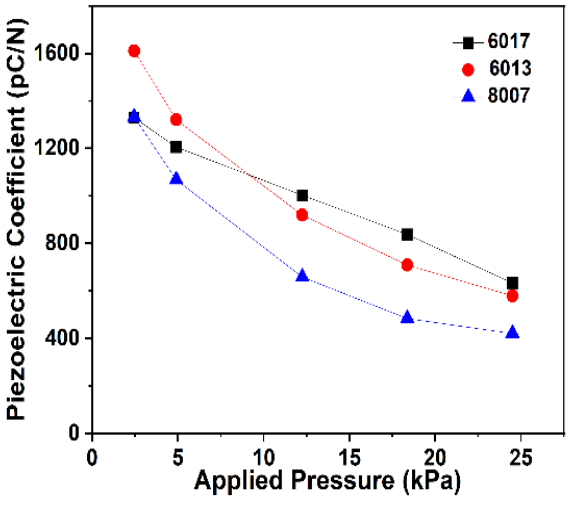

Fig. 2 Quasi-static piezoelectric coefficient of piezoelectret from COC 6017, 6013, and 8007.

The perceived discrepancy might be due to the variations between the samples when manually aligning and assembling the layers during fabrication. The piezoelectric coefficient d_{33} is related to the surface charge σ and the modulus of the structure Y, following the following equation[51, 52]

$$d_{33} = k\frac{\sigma}{Y} \quad (3)$$

where k is a parameter that is related to the dielectric constants of the materials and piezoelectrets' porous structures. As all three COCs had very similar dielectric properties, and the piezoelectrets had the same designed porous structure, both k and Y would be similar among all three piezoelectrets. The d_{33}would be similar among the piezoelectrets from different COCs, provided that the surface charge densities were similar under the same charging conditions. While the charging behaviors will be discussed later in this paper, the surface charge densities among the three piezoelectrets were very similar when charged at the same voltage.

3.2 Thermally stability of electrical charges

Figure 3 shows the results of the thermal stability of the three COC piezoelectrets measured by thermally stimulated discharge (TSD). The main discharge peaks for 6017, 6013, and 8007 were around 210 °C, 180 °C, and 130 °C, respectively. The discharge peak temperatures were ~30-50 °C higher than the respective glass transition temperature of the three COC materials, which were consistent with previous studies.[20,22,27] It is worth noting that the discharge temperatures of 6017 and 6013, and even 8007 were significantly higher than the working temperature of typical commercialized piezoelectric foams, such as PP piezoelectric foams (70~80°C).[37,40]

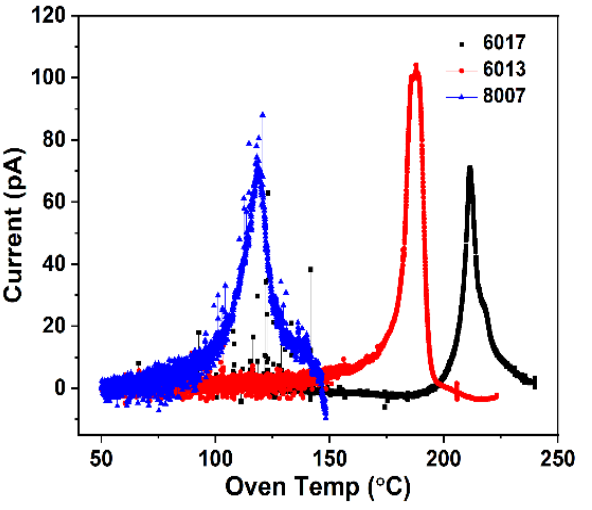

Fig. 3 Thermally stimulated discharge of three types of COC piezoelectret.

Aside from the main peak, a series of scattered discharges at lower temperatures were also observed with a minor second discharge peak for COC 6017 and 6013. This peak was attributed to the unstable charges, while the main peak was related to the discharge of stable charges. This 'discrete discharge' peak was located in the same temperature range for both COC 6017 and 6013. For COC 8007 piezoelectrets, only a single peak was observed, plausibly from the convoluted signals from both stable and unstable charges, because of the significantly lower glass transition temperature and lower thermal stability of the stable charges.

Table 2 shows the percentage of stable and unstable charges in different piezoelectrets obtained by integrating current overtime followed by normalizing the peak charge against the total charge. For COC 8007 piezoelectrets, the signals of stable and unstable charges were convoluted together, which made calculations impossible. Despite the sample-to-sample differences, qualitatively, it could be argued that in 6017 piezoelectrets, unstable charges account for ~10% and stable charges account for ~90% of total charges. Both fractions were comparable to those in COC 6013 piezoelectret.

Table 2. Percentage of stable and unstable charge in different piezoelectrets.

COC Type	Unstable Charge	Stable Charge	Total Charge
6013	7.4%	92.6%	100%
6017a	5.8% ~13.5%	86.5% ~94.2%	100%
8007	N/A	N/A	100%

[a]:calculations were conducted using data from multiple measurements.

3.3 Electrical and electromechanical properties of COC piezoelectrets

The electrical polarization and charge buildup in the COC piezoelectret were investigated by hysteresis loop. Fig. 4 shows the applied ac-bias voltage on the surface of the sample over time during the electric hysteresis loop measurements. The same voltage profiles were applied in the measurements of all three COC piezoelectrets.

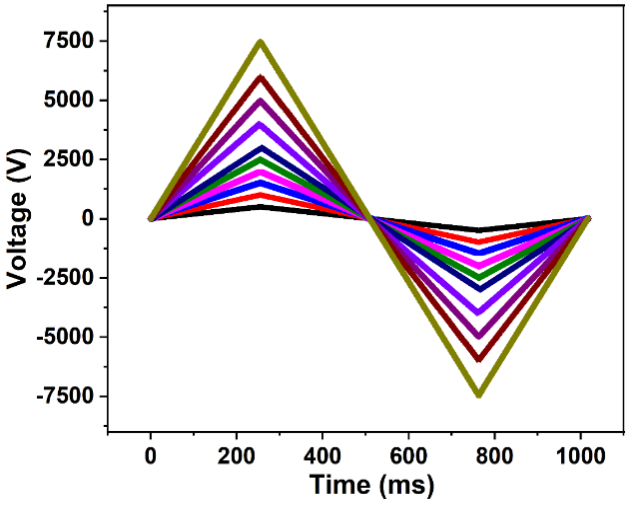

Fig. 4 Voltage profiles for electrical hysteresis measurements.

Figure 5 shows the hysteresis loop of the three samples, which are similar to each other. Fig. 6 shows the charge build-up in the artificial void of the samples. The quasi-permanent polarization for the three samples was derived from their respective hysteresis loop. The three COC piezoelectrets showed almost identical polarization behaviors. The breakdown occurred at about 2500 V, after which the polarization increased almost linearly with increasing voltage.

In the charging of the samples, the discharge takes place via dielectric barrier discharge.[57] Using a layer model,[22] the relationship between the breakdown voltage and the geometric parameters was derived.[50]

$$V_{bd} = \frac{ap}{ln(ph_{air})+b}\left(\frac{h_{COC}}{\varepsilon_{COC}} + 2h_{air}\right) \quad (4)$$

where V_{bd} is the breakdown threshold voltage, a equals 4.36×10^7 V/(atm·m), p is gas pressure (1atm in the study), d is the thickness of gas (50.8μm in this study), b equals 12.8, h_{air}, and h_{COC} is the thickness of single air bubble height and the total thickness of COC respectively, $\boldsymbol{\varepsilon}_{COC}$ is the relative permittivity of COC.

The model's prediction of breakdown voltage was only related to the geometric structure of the material given certain charging conditions. As the piezoelectret from different materials have the same geometry, the breakdown voltage predicted would be the same. Equation (4) yielded a predicted breakdown voltage of 3141V, which was slightly higher than

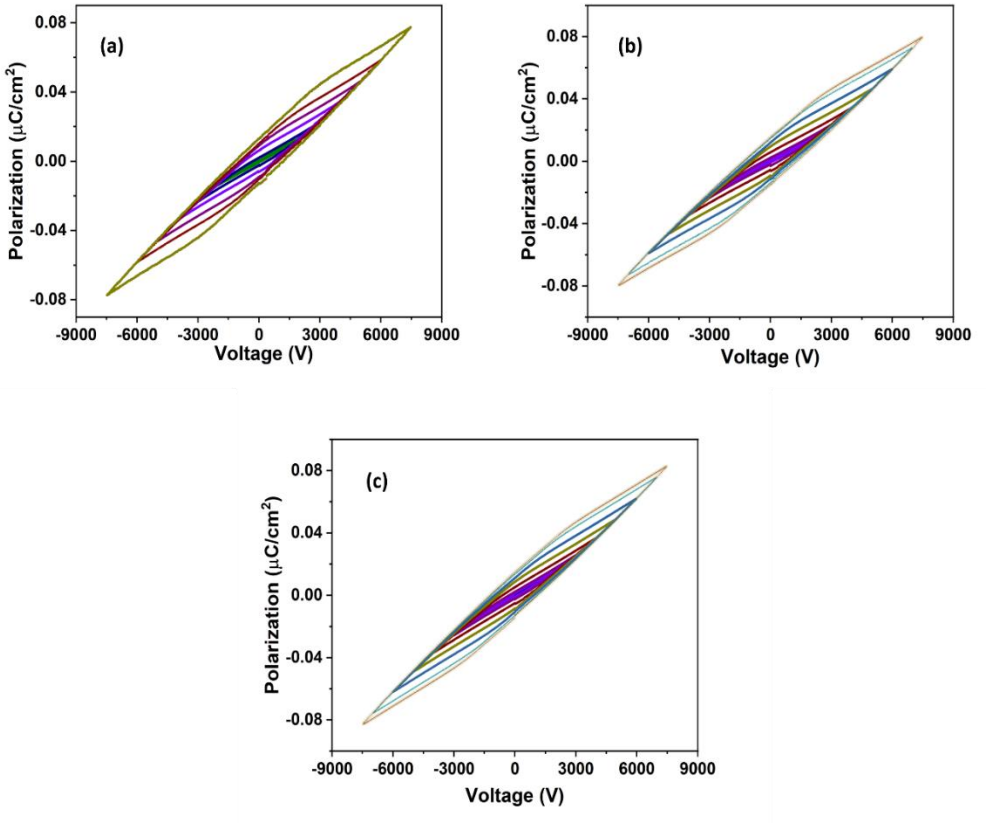

Fig. 5 Hysteresis loop of the prepared sample (a). 6017 (b). 6013 (c). 8007.

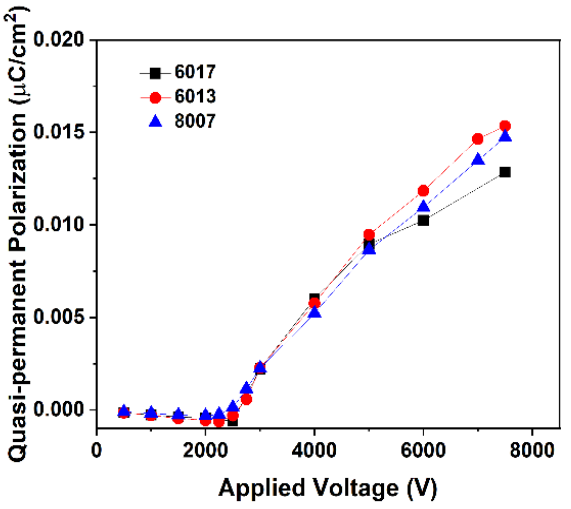

Fig. 6 Quasi-static charge builds up in the artificial void.

2500V. As previously discussed,[50] this might be due to the deflection of the sample structure during the CO_2 bonding. The deflection would reduce the air gap and cause a decrease in the breakdown voltage (Equation 4).

Upon exceeding the breakdown threshold voltage, the quasi-permanent charge continuously built up in all three piezoelectrets and showed almost identical linear dependency with increasing voltage. This indicates that back discharge did not take place in the applied voltage range.

From the quasi-permanent charge, the charge density inside the artificial void can be also calculated. With a 5000V charging voltage, the charge density, which equals the value of quasi-permanent polarization, is approximately 0.087μC/cm^2. With a 4 cm^2 electrode used in this experiment, the total amount of charge stored can be calculated to be 34800pC. By comparison, the total charge obtained from the thermally stimulated discharge test was 29000pC.

The higher total charge obtained by hysteresis loop testing was probably due to the stored charges not being fully released during TSD. In addition, a tiny leak current may also play a role during the hysteresis loop test even though samples were carefully treated to prevent a leak current. Nevertheless, overall, the total charge from the two measurements was comparable. The result also showed that the hysteresis loop was dominated by the piezoelectric effect with space charge, not by the leak current described in the literature.[58]

Figure 7 shows the butterfly loop of 6017, 6013, and 8007 piezoelectrets, respectively. The traces were of "real" butterfly loops with a clockwise orientation on the right part, which is characteristic of behavior dominated by piezoelectric behavior

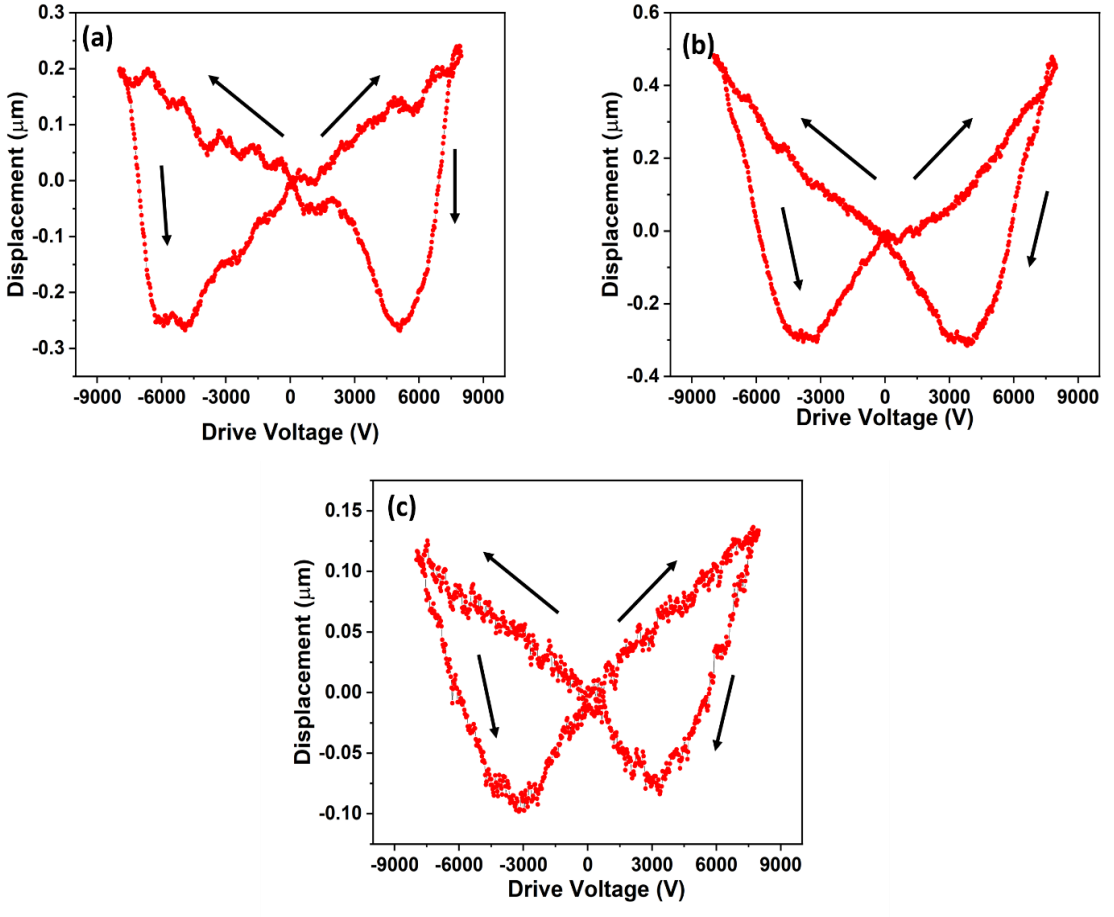

Fig. 7 Butterfly loop for (a). 6017 (b). 6013 (c). 8007 piezoelectrets.

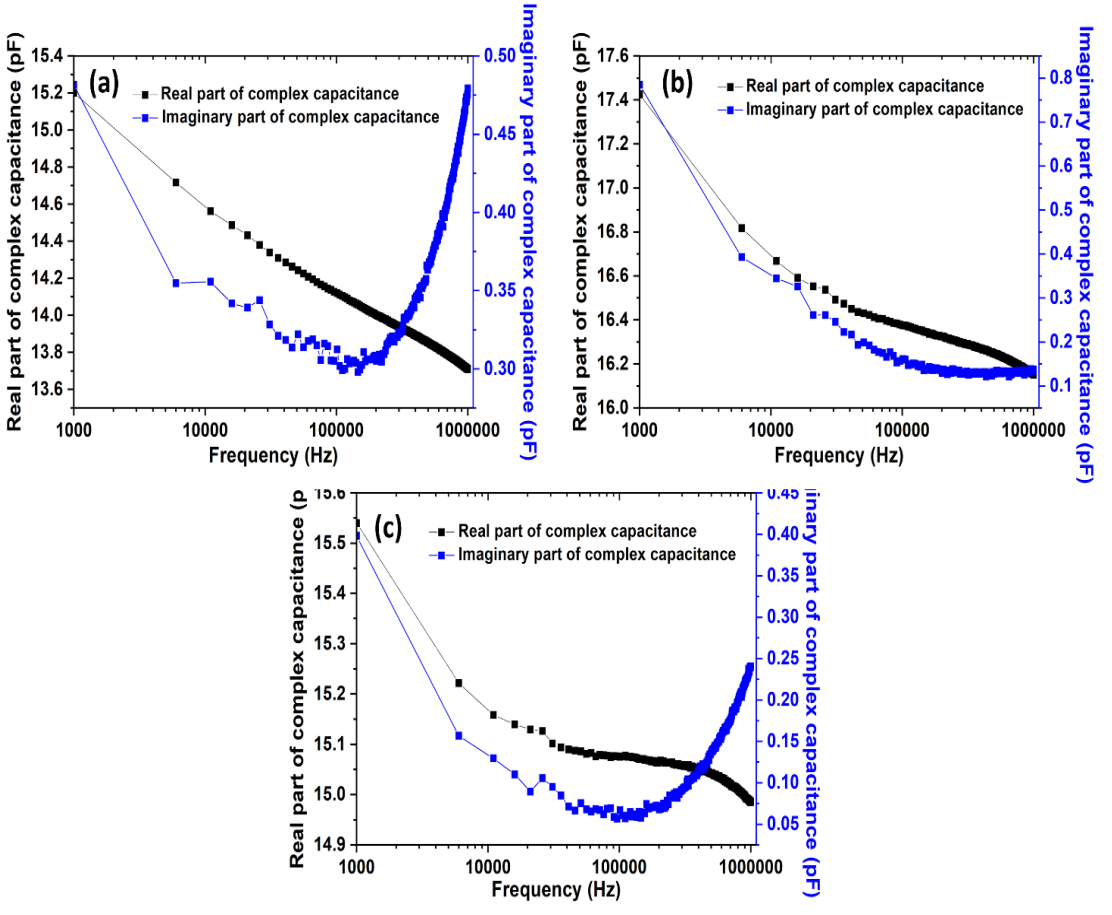

Fig. 8 Dielectric spectrum of the material (a). Sample fabricated by COC 6017 (b). Sample fabricated by COC 6013 (c). Sample fabricated by COC 8007.

rather than elastic compliance of the materials as reported in the literature.[59] From the graph, the inverse piezoelectric coefficient of 6017, 6013, and 8007 can be calculated as 25 pm/V, 40 pm/V, and 15 pm/V, respectively, which are similar to other piezoelectric materials such as PZT material.[60,61] Considering the sample-to-sample variation during fabrication, it is plausible that the inverse piezoelectric coefficient of the three types of material is similar. The inverse piezoelectric coefficient was significantly lower than the piezoelectric coefficient, resulting from the different responses of the non-overlapping structure to mechanical and electrical force and much smaller deformation under electrical excitation.[50]

To further understand the dielectric properties[62-66] and the resonance behavior of the piezoelectrets, dielectric resonance spectroscopy[67] was conducted. Fig. 8 shows the measured results. Contrary to typical piezoelectric materials and piezoelectrets reported in the literature, no resonance peak was observed for any of the COC piezoelectrets. This phenomenon also resulted from the unique response of the non-overlapping structure to the electrical force, which may be understood from the following.

During the dielectric resonance spectrum analysis, the sample is under forced vibrations with damping effects under a harmonic excitation force from the applied electric field. The system may be represented by a single degree of freedom (sdof) linear oscillator illustrated in Fig. 9. The equation of motion for the system can be simplified to:

$$m\ddot{x} + \gamma\dot{x} + kx = F_0 \cos\omega t \quad (5)$$

Where m is the mass of the system, γ is the damping coefficient, k is the spring constant, ω is the frequency and t is time. $F_0 \cos\omega t$ is the harmonic excitation the sample experienced during the experiment, and F_0 is the amplitude of the driving force. Let $\xi = \frac{\gamma}{2\omega_0 m}$, $\omega_0^2 = \frac{k}{m}$, where ξ is the damping ratio, ω_0 is the natural frequency of the system without damping.

When the amplitude resonance occurs, the maximum amplitude is determined by:

$$A_{resonance} = \frac{F_0/k}{2\xi\sqrt{1-\xi^2}} \quad (6)$$

During the dielectric resonance spectra measurements, the electrical force is uniformly exerted on the middle layer of solid COC film (Fig. 10). This is, effectively, to uniformly compress the solid COC polymer with high modulus and

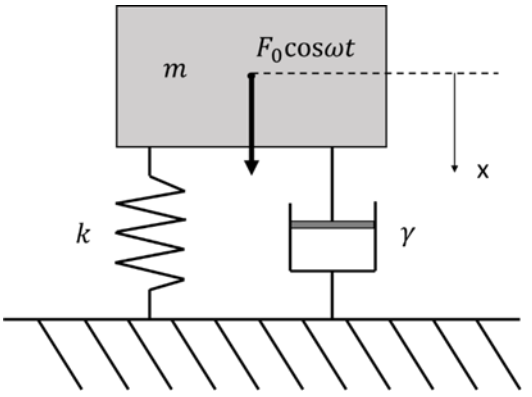

Fig. 9 Schematic of a single degree of freedom (sdof) linear oscillator.

would result in a system with very high spring constant k. Moreover, as the COC film was fixed to the underneath solid ridges on either side, it is conceivable that such restriction would cause the strain response to lag and be out of phase with the applied force. This effect would be the most severe at either end and become less toward the center of the film. Such a lag effectively indicates the system possesses a large damping ratio and energy dissipation. According to Equation (6), a high spring constant and damping ratio results in a diminished amplitude not observable in experiments. As the Quality Factor of the system:

$$Q = \frac{1}{2\xi} = 2\pi \times \frac{Energy\ Stored}{Energy\ Dissipated}(per\ cycle) \qquad (7)$$

The system also has a small Q-factor and is losing energy fast, and the resonance peak will not be observed. A larger mechanical vibration excitation may be necessary in the future to determine the resonance and anti-resonance frequency instead of electrical force-based excitation.[68]

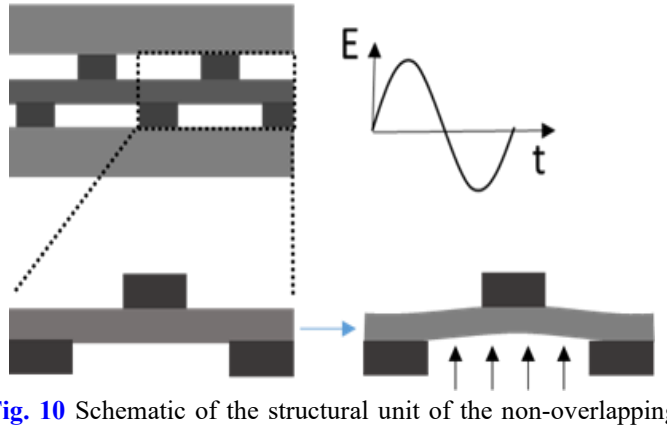

Fig. 10 Schematic of the structural unit of the non-overlapping structure and its deformation in response to electrical excitation.

4. Conclusion

This study examined piezoelectrets prepared with three COC materials with similar dielectric properties but different thermal stability and mechanical properties. All piezoelectrets displayed good piezoelectric activity, and a high piezoelectric coefficient of approximately 1600pC/N was obtained. The thermal stability of the piezoelectrets was investigated and found to correlate well with the glass transition temperatures of the materials. The charge build-up process inside the artificial void of the structure was measured by the hysteresis loop measurement and compared. It was found that the charging behaviors among the piezoelectrets were similar and were decided by the geometry of the voids. A charging threshold voltage of about 2500V remained the same for all three materials and was in good agreement with the layer model prediction. The piezoelectrets exhibited piezoelectric effect-dominated butterfly loop behaviors. While effective in improving the piezoelectric d_{33} and beneficial for sensor activity, the non-overlapping structure employed in the piezoelectrets resulted in a high damping ratio and high energy dissipation under electrical excitation. This leads to the substantially lower inverse piezoelectric coefficients (calculated from the butterfly loops) and the absence of resonance peaks in the dielectric spectra measurements. The COC piezoelectrets prepared in this study possessed different mechanical/thermal properties combinations and similar piezoelectric properties and can potentially be used for sensing and other applications under a broad range of conditions.

Acknowledgment

We thank Dr. William Oates of the Mechanical Engineering Department of FAMU-FSU College of Engineering, for the discussion on the electromechanical characterization and modeling of the COC piezoelectrets.

Conflict of Interest

There is no conflict of interest.

Supporting Information

Not applicable.

References

[1] T. Gong, M.-Q. Liu, H. Liu, S.-P. Peng, T. Li, R.-Y. Bao, W. Yang, B.-H. Xie, M.-B. Yang, Z. Guo, Selective distribution and migration of carbon nanotubes enhanced electrical and mechanical performances in polyolefin elastomers, *Polymer*, 2017, **110**, 1-11, doi: 10.1016/j.polymer.2016.12.056.

[2] H. Zhang, Y. B. Chong, Y. Zhao, A. Buryak, F. Duan, J. Yang, Self-Sealing Polyolefin by Super-Absorbent Polymer, *Engineered Science*, 2019, **8**, 66-75, doi: 10.30919/es8d801.

[3] G. Han, Y.-F. Su, S. Ma, T. Nantung, N. Lu, in situ rheological properties monitoring of cementitious materials through the piezoelectric-based electromechanical impedance (EMI) approach, *Engineered Science*, 2021, **16**, 259-268, doi:

10.30919/es8d537.
[4] D. Pan, F. Su, H. Liu, C. Liu, A. Umar, L. Castañeda, H. Algadi, C. Wang, Z. Guo, Research progress on catalytic pyrolysis and reuse of waste plastics and petroleum sludge, *ES Materials & Manufacturing*, 2021, **11**, 3-15, doi: 10.30919/esmm5f415.
[5] D. Zou, S. Liu, C. Zhang, Y. Hong, G. Zhang, Z. Yang, Flexible and translucent PZT films enhanced by the compositionally graded heterostructure for human body monitoring, *Nano Energy*, 2021, **85**, 105984, doi: 10.1016/j.nanoen.2021.105984.
[6] K.-I. Park, J. H. Son, G.-T. Hwang, C. K. Jeong, J. Ryu, M. Koo, I. Choi, S. H. Lee, M. Byun, Z. L. Wang, K. J. Lee, Highly-efficient, flexible piezoelectric PZT thin film nanogenerator on plastic substrates, *Advanced Materials*, 2014, **26**, 2514-2520, doi: 10.1002/adma.201305659.
[7] Y.-F. Su, G. Han, Z. Kong, T. Nantung, N. Lu, Embeddable piezoelectric sensors for strength gain monitoring of cementitious materials: the influence of coating materials, *Engineered Science*, 2020, **11**, 66-75, doi: 10.30919/es8d1114.
[8] Z. Wang, Z. Liu, G. Zhao, Z. Zhang, X. Zhao, X. Wan, Y. Zhang, Z. L. Wang, L. Li, Stretchable unsymmetrical piezoelectric $BaTiO_3$ composite hydrogel for triboelectric nanogenerators and multimodal sensors, *ACS Nano*, 2022, **16**, 1661-1670, doi: 10.1021/acsnano.1c10678.
[9] B. Xun, A. Song, J. Yu, Y. Yin, J.-F. Li, B.-P. Zhang, Lead-free $BiFeO_3$-$BaTiO_3$ ceramics with high curie temperature: fine compositional tuning across the phase boundary for high piezoelectric charge and strain coefficients, *ACS Applied Materials & Interfaces*, 2021, **13**, 4192-4202, doi: 10.1021/acsami.0c20381.
[10] A. Savolainen, K. Kirjavainen, Electrothermomechanical film, Part I. design and characteristics, *Journal of Macromolecular Science: Part A - Chemistry*, 1989, **26**, 583-591, doi: 10.1080/00222338908051994.
[11] W. Wirges, M. Wegener, O. Voronina, L. Zirkel, R. Gerhard-Multhaupt, Optimized preparation of elastically soft, highly piezoelectric, cellular ferroelectrets from nonvoided poly(ethylene terephthalate) films, *Advanced Functional Materials*, 2007, **17**, 324-329, doi: 10.1002/adfm.200600162.
[12] M. Wegener, W. Wirges, R. Gerhard-Multhaupt, Piezoelectric polyethylene terephthalate (PETP) foams - specifically designed and prepared ferroelectret films, *Advanced Engineering Materials*, 2005, **7**, 1128-1131, doi: 10.1002/adem.200500177.
[13] N. Behrendt, Tailored processing methods for cellular polycarbonate and polyetherimide films - new potentials for electret and piezoelectric applications, *IEEE Transactions on Dielectrics and Electrical Insulation*, 2010, **17**, 1113-1122, doi: 10.1109/TDEI.2010.5539682.
[14] N. Behrendt, C. Greiner, F. Fischer, T. Frese, V. Altstädt, H.-W. Schmidt, R. Giesa, J. Hillenbrand, G. M. Sessler, Morphology and electret behaviour of microcellular high glass temperature films, *Applied Physics A*, 2006, **85**, 87-93, doi: 10.1007/s00339-006-3660-7.
[15] X. Qiu, L. Holländer, R. F. Suárez, W. Wirges, R. Gerhard, Polarization from dielectric-barrier discharges in ferroelectrets: mapping of the electric-field profiles by means of thermal-pulse tomography, *Applied Physics Letters*, 2010, **97**, 072905, doi: 10.1063/1.3481802.
[16] F. Peng, H. Lars, W. Werner, G. Reimund, Measurement Science and Technology, Piezoelectric d_{33} coefficients in foamed and layered polymer piezoelectrets from dynamic mechano-electrical experiments, electro-mechanical resonance spectroscopy and acoustic-transducer measurements, *Measurement Science and Technology*, 2012, **23**, 035604, doi: 10.1088/0957-0233/23/3/035604.
[17] F. Peng, Q. Xunlin, W. Wirges, R. Gerhard, L. Zirkel, Polyethylene-naphthalate (PEN) Ferroelectrets: Cellular Structure, Piezoelectricity and Thermal Stability, *IEEE Transactions on Dielectrics and Electrical Insulation*, 2010, **17**, 1079-1087, doi: 10.1109/TDEI.2010.5539678.
[18] P. Fang, W. Wirges, M. Wegener, L. Zirkel, R. Gerhard, Cellular polyethylene-naphthalate films for ferroelectret applications: foaming, inflation and stretching, assessment of electromechanically relevant structural features, *e-Polymers*, 2008, **8**, 487-495, doi: 10.1515/epoly.2008.8.1.487.
[19] P. Fang, M. Wegener, W. Wirges, R. Gerhard, L. Zirkel, Cellular polyethylene-naphthalate ferroelectrets: Foaming in supercritical carbon dioxide, structural and electrical preparation, and resulting piezoelectricity, *Applied Physics Letters*, 2007, **90**, 192908, doi: 10.1063/1.2738365.
[20] X. Zhang, G. M. Sessler, Y. Wang, Fluoroethylenepropylene ferroelectret films with cross-tunnel structure for piezoelectric transducers and micro energy harvesters, *Journal of Applied Physics*, 2014, **116**, 074109, doi: 10.1063/1.4893367.
[21] R. Pisani Altafim, D. Rychkov, W. Wirges, R. Gerhard, H. Basso, R. Correa Altafim, M. Melzer, Laminated tubular-channel ferroelectret systems from low-density polyethylene films and from fluoroethylene- propylene copolymer films - A comparison, *IEEE Transactions on Dielectrics and Electrical Insulation*, 2012, **19**, 1116-1123, doi: 10.1109/tdei.2012.6259978.
[22] Z. Sun, X. Zhang, Z. Xia, X. Qiu, W. Wirges, R. Gerhard, C. Zeng, C. Zhang, B. Wang, Polarization and piezoelectricity in polymer films with artificial void structure, *Applied Physics A*, 2011, **105**, 197-205, doi: 10.1007/s00339-011-6481-2.
[23] X. Zhang, G. Cao, Z. Sun, Z. Xia, Fabrication of fluoropolymer piezoelectrets by using rigid template: structure and thermal stability, *Journal of Applied Physics*, 2010, **108**, 064113, doi: 10.1063/1.3482011.
[24] R. Alberto Pisani Altafim, X. Qiu, W. Wirges, R. Gerhard, R. Alberto Corrêa Altafim, H. C. Basso, W. Jenninger, J. Wagner, Template-based fluoroethylenepropylene piezoelectrets with tubular channels for transducer applications, *Journal of Applied Physics*, 2009, **106**, 014106, doi: 10.1063/1.3159039.
[25] O. Voronina, M. Wegener, W. Wirges, R. Gerhard, L. Zirkel, H. Münstedt, Physical foaming of fluorinated ethylene-propylene (FEP) copolymers in supercritical carbon dioxide: single-film fluoropolymer piezoelectrets, *Applied Physics A*, 2008, **90**, 615-618, doi: 10.1007/s00339-007-4371-4.

[26] J. Huang, X. Zhang, Z. Xia, X. Wang, Piezoelectrets from laminated sandwiches of porous polytetrafluoroethylene films and nonporous fluoroethylenepropylene films, *Journal of Applied Physics*, 2008, **103**, 084111, doi: 10.1063/1.2910773.
[27] X. Zhang, J. Hillenbrand, G. M. Sessler, Ferroelectrets with improved thermal stability made from fused fluorocarbon layers, *Journal of Applied Physics*, 2007, **101**, 054114, doi: 10.1063/1.2562413.
[28] Altafim, Basso, Altafim, Lima, D. Aquino, Neto, Gerhard-Multhaupt, Piezoelectrets from thermo-formed bubble structures of fluoropolymer-electret films, *IEEE Transactions on Dielectrics and Electrical Insulation*, 2006, **13**, 979-985, doi: 10.1109/tdei.2006.247822.
[29] X. Zhang, P. Pondrom, G. M. Sessler, X. Ma, Ferroelectret nanogenerator with large transverse piezoelectric activity, *Nano Energy*, 2018, **50**, 52-61, doi: 10.1016/j.nanoen.2018.05.016.
[30] B. Gustavo Ortega, S. Pedro Llovera, M. Francisco, Q. Alfredo, Influence of corona charging in cellular polyethylene film, *Journal of Physics: Conference Series*, 2011, **301**, 012054, doi: 10.1088/1742-6596/301/1/012054.
[31] Z. Xiaoqing, Z. Xinwu, M. S. Gerhard, G. Xiangshan, Quasi-static and dynamic piezoelectric responses of layered polytetrafluoroethylene ferroelectrets, *Journal of Physics D: Applied Physics*, 2014, **47**, 015501, doi: 10.1088/0022-3727/47/1/015501.
[32] R. Gerhard-Multhaupt, W. Kunstler, T. Gome, A. Pucher, T. Weinhold, M. Seiss, Z. Xia, A. Wedel, R. Danz, Porous PTFE space-charge electrets for piezoelectric applications, *IEEE Transactions on Dielectrics and Electrical Insulation*, 2000, **7**, 480-488, doi: 10.1109/94.868065.
[33] X. Zhang, X. Zhang, Q. You, G. M. Sessler, Low-cost, large-area, stretchable piezoelectric films based on irradiation-crosslinked poly(propylene), *Macromolecular Materials and Engineering*, 2014, **299**, 290-295, doi: 10.1002/mame.201300161.
[34] X. Zhang, J. Huang, J. Chen, Z. Wan, S. Wang, Z. Xia, Piezoelectric properties of irradiation-crosslinked polypropylene ferroelectrets, *Applied Physics Letters*, 2007, **91**, 182901, doi: 10.1063/1.2803316.
[35] A. Mellinger, M. Wegener, W. Wirges, R. R. Mallepally, R. Gerhard-Multhaupt, Thermal and temporal stability of ferroelectret films made from cellular polypropylene/air composites, *Ferroelectrics*, 2006, **331**, 189-199, doi: 10.1080/00150190600737933.
[36] J. Hillenbrand, G. M. Sessler, High-sensitivity piezoelectric microphones based on stacked cellular polymer films (L), *The Journal of the Acoustical Society of America*, 2004, **116**, 3267-3270, doi: 10.1121/1.1810272.
[37] M. Paajanen, J. Lekkala, H. Valimaki, Electromechanical modeling and properties of the electret film EMFI, *IEEE Transactions on Dielectrics and Electrical Insulation*, 2001, **8**, 629-636, doi: 10.1109/94.946715.
[38] G. S. Neugschwandtner, R. Schwödiauer, M. Vieytes, S. Bauer-Gogonea, S. Bauer, J. Hillenbrand, R. Kressmann, G. M. Sessler, M. Paajanen, J. Lekkala, Large and broadband piezoelectricity in smart polymer-foam space-charge electrets, *Applied Physics Letters*, 2000, **77**, 3827-3829, doi: 10.1063/1.1331348.
[39] R. H. Ali Samadi, Taher Azdast, Hossein Abdollahi, Payam Zarrintaj, Mohammad Reza Saeb, Piezoelectric performance of microcellular polypropylene foams fabricated using foam injection molding as a potential scaffold for bone tissue engineering, *Journal of Macromolecular Science, Part B*, 2020, **59**, 14, doi: 10.1080/00222348.2020.1730573.
[40] M. Paajanen, J. Lekkala, K. Kirjavainen, ElectroMechanical Film (EMFi)—a new multipurpose electret material, *Sensors and Actuators A: Physical*, 2000, **84**, 95-102, doi: 10.1016/s0924-4247(99)00269-1.
[41] K. Sappati, S. Bhadra, Piezoelectric polymer and paper substrates: a review, *Sensors*, 2018, 18, 3605, doi: 10.3390/s18113605.
[42] G.M. Sessler, G. M. Yang, W. Hakte, Electret properties of cycloolefin copolymers, *Electrical Insulation and Dielectric Phenomena*, 1997, **2**, 467-470, doi: 10.1109/CEIDP.1997.641113.
[43] G. C. Montanari, D. Fabiani, F. Ciani, A. Motori, M. Paajanen, R. Gerhard-Multhaupt, M. Wegener, Charging properties and time-temperature stability of innovative polymeric cellular ferroelectrets, *IEEE Transactions on Dielectrics and Electrical Insulation*, 2007, **14**, 238-248, doi: 10.1109/tdei.2007.302892.
[44] Saarimaki, Paajanen, Savijarvi, Minkkinen, Wegener, Voronina, Schulze, Wirges, Gerhard-Multhaupt, Novel heat durable electromechanical film: processing for electromechanical and electret applications, *IEEE Transactions on Dielectrics and Electrical Insulation*, 2006, **13**, 963-972, doi: 10.1109/tdei.2006.247820.
[45] M. Wegener, M. Paajanen, O. Voronina, R. Schulze, W. Wirges, R. Gerhard-Multhaupt, Voided cyclo-olefin polymer films: ferroelectrets with high thermal stability, *International Symposium on Electrets*, Salvador, Brazil, 2005, 47-50, doi: 10.1109/ISE.2005.1612315.
[46] A.M. Savijarvi, M. Paajanen, E. Saarimaki, H. Minkkinen, Novel heat durable electromechanical films: cellular film making from cyclic olefin polymers, *12th International Symposium on Electrets*, Salvador, Brazil, 2005, 75-78, doi: 10.1109/ISE.2005.1612322.
[47] Y. L. H. Wang, X. Wang, Z. Liu, M. Fasial, C. Zeng, Preparation and characterization of piezoelectric foams based on cyclic olefin copolymer, *Engineered Science*, 2021, **16**, 203-210, doi: 10.30919/es8d560.
[48] TOPAS Cyclic Olefin Copolymer data sheet, url: http://www.topas.com/sites/default/files/files/TOPAS_Brochure_E_2014_06(1).pdf
[49] Y. Li, C. Zeng, Low-temperature CO_2-assisted assembly of cyclic olefin copolymer ferroelectrets of high piezoelectricity and thermal stability, *Macromolecular Chemistry and Physics*, 2013, **214**, 2733-2738, doi: 10.1002/macp.201300440.
[50] G. Buchberger, R. Schwödiauer, S. Bauer, Flexible large area ferroelectret sensors for location sensitive touchpads, *Applied Physics Letters*, 2008, **92**, 123511, doi: 10.1063/1.2903711.

[51] G. M. Sessler, J. Hillenbrand, Electromechanical response of cellular electret films, *Applied Physics Letters*, 1999, **75**, 3405-3407, doi: 10.1063/1.125308.
[52] J. Hillenbrand, G. M. Sessler, Piezoelectricity in cellular electret films, *IEEE Transactions on Dielectrics and Electrical Insulation*, 2000, **7**, 537-542, doi: 10.1109/94.868074.
[53] A. I. Cooper, Polymer synthesis and processing using supercritical carbon dioxide, *Journal of Materials Chemistry*, 2000, **10**, 207-234, doi: 10.1039/a906486i.
[54] D. L. Tomasko, H. Li, D. Liu, X. Han, M. J. Wingert, L. J. Lee, K. W. Koelling, A review of CO_2 applications in the processing of polymers, *Industrial & Engineering Chemistry Research*, 2003, **42**, 6431-6456, doi: 10.1021/ie030199z.
[55] C. Gongxun, Z. Xiaoqing, Z. Da, C. Zhang, W. Ben, Z. Changchun, Charge storage and transport in oriented and non-oriented polytetrafluoroethylene films, *IEEE Transactions on Dielectrics and Electrical Insulation*, 2012, **19**, 1108-1115, doi: 10.1109/TDEI.2012.6259977.
[56] A. Mellinger, Dielectric resonance spectroscopy: a versatile tool in the quest for better piezoelectric polymers, *IEEE Transactions on Dielectrics and Electrical Insulation*, 2003, **10**, 842-861, doi: 10.1109/TDEI.2003.1237333.
[57] M. Wegener, S. Bauer, Microstorms in cellular polymers: a route to soft piezoelectric transducer materials with engineered macroscopic dipoles, *ChemPhysChem*, 2005, **6**, 1014-1025, doi: 10.1002/cphc.200400517.
[58] J. F. Scott, Ferroelectrics go bananas, *Journal of Physics: Condensed Matter*, 2008, **20**, 021001, doi: 10.1088/0953-8984/20/02/021001.
[59] R. Schwodiauer, I. Graz, S. Bauer, Charging and switching of ferroelectrets. How much can ferroelectrets behave like ferroelectrics? 14th IEEE International Symposium on Applications of Ferroelectrics, 2004, ISAF-04 2004, Montreal, QC, Canada, 2004, 134-137, doi: 10.1109/ISAF.2004.1418355.
[60] S. Xie, A. Gannepalli, Q. N. Chen, Y. Liu, Y. Zhou, R. Proksch, J. Li, High resolution quantitative piezoresponse force microscopy of $BiFeO_3$ nanofibers with dramatically enhanced sensitivity, *Nanoscale*, 2012, **4**, 408-413, doi: 10.1039/c1nr11099c.
[61] M. Hinterstein, J. Rouquette, J. Haines, P. Papet, M. Knapp, J. Glaum, H. Fuess, Structural description of the macroscopic piezo- and ferroelectric properties of lead zirconate titanate, *Physical Review Letters*, 2011, **107**, 077602, http://link.aps.org/doi/10.1103/PhysRevLett.107.077602.
[62] J. Wang, Z. Shi, X. Wang, X. Mai, R. Fan, H. Liu, X. Wang, Z. Guo, Enhancing dielectric performance of poly(vinylidene fluoride) nanocomposites via controlled distribution of carbon nanotubes and barium titanate nanoparticle, *Engineered Science*, 2018, **4**, 79-86, doi: 10.30919/es8d759.
[63] Z. Zheng, O. Olayinka, B. Li, 2S-soy protein-based biopolymer as a non-covalent surfactant and its effects on electrical conduction and dielectric relaxation of polymer nanocomposites, *Engineered Science*, 2018, **4**, 87-99, doi: 10.30919/es8d766.
[64] H. R. Tian, C. F. Xing, H. T. Wu, Z. H. Wang, Behavior and Microwave Dielectric Properties of Low-Loss $Li_6Mg_7Zr_3O_{16}$ Ceramics Doped with Different LiF Additives, *ES Materials & Manufacturing*, 2019, **6**, 18-23, doi: 10.30919/esmm5f603.
[65] L. Sun, L. Liang, Z. Shi, H. Wang, P. Xie, D. Dastan, K. Sun, R. Fan, Optimizing strategy for the dielectric performance of topological-structured polymer nanocomposites by rationally tailoring the spatial distribution of nanofillers, *Engineered Science*, 2020, **12**, 95-105, doi: 10.30919/es8d1148.
[66] Y. Zhou, P. Wang, G. Ruan, P. Xu, Y. Ding, Synergistic effect of P[MPEGMA-IL]modified graphene on morphology and dielectric properties of PLA/PCL blends, *ES Materials & Manufacturing*, 2021, **11**, 20-29, doi: 10.30919/esmm5f928.
[67] A. Mellinger, Dielectric resonance spectroscopy: a versatile tool in the quest for better piezoelectric polymers, *IEEE Transactions on Dielectrics and Electrical Insulation*, 2003, **10**, 842-861, doi: 10.1109/Tdei.2003.1237333.
[68] P. Pondrom, J. Hillenbrand, G. M. Sessler, J. Bos, T. Melz, Energy harvesting with single-layer and stacked piezoelectret films, *IEEE Transactions on Dielectrics and Electrical Insulation*, 2015, **22**, 1470-1476, doi: 10.1109/tdei.2015.7116339.